Bohm's quantum-force time series: Stable distribution, flat power spectrum, and implication

Boon Leong Lan
School of Engineering and Science, Monash University, P.O. Box 8975, 46780 Petaling Jaya, Selangor, Malaysia

(Received 21 December 1999; revised manuscript received 27 September 2000; published 16 March 2001)

New insight into the nature of Bohm's quantum force is presented. Based on our numerical study, we conclude that, for the kicked pendulum, Bohm's quantum-force time-series for nonstationary states is *typically* or *generically* non-Gaussian stable distributed with a flat power spectrum. For fixed system parameters and initial wave function, the stable parameters and the constant value of the power spectrum are independent of the initial Bohmian angle. We conjecture that these properties of the quantum-force time-series are also typical or generic for other classically chaotic Hamiltonian dynamical systems since the kicked pendulum is a prototypical member of this class of systems. A new method of calculating the quantum probability density of a particle's position implied by these quantum-force properties is described.

DOI: 10.1103/PhysRevA.63.042105 PACS number(s): 03.65.Ta, 05.45.−a

I. INTRODUCTION

According to Bohm's [1] causal ontological interpretation of quantum theory, matter, independent of observers, has a well-defined trajectory that is defined by the equation [1,2]

$$\frac{dx(t)}{dt}=\frac{1}{m}\nabla S(x,t)\bigg|_{x(t)},\qquad (1)$$

where $x(t)$ is the position of the particle, m is the mass, and $S(x,t)$ is the phase of the quantum wave function

$$\psi(x,t)=R(x,t)\exp[iS(x,t)/\hbar]\qquad (2)$$

that time evolves according to the time-dependent Schrodinger's equation. In order to solve the first-order differential equation Eq. (1) for the Bohmian position $x(t)$, not only must the initial position x_0 be specified but also the initial wave function $\psi_0(x)$ because the time-dependent Schrodinger's equation has to be solved to obtain $S(x,t)$. Once $x(t)$ and $S(x,t)$ are known, the momentum of the particle is determined using Eq. (1)

$$p(t)=\nabla S(x,t)|_{x(t)}.\qquad (3)$$

Now, substituting Eq. (2) into the time-dependent Schrodinger's equation leads to two equations, one from the real part of the equation and the other from the imaginary part. The former equation, with the use of Eq. (1), leads to an equation that has the form of Newton's second law [1,2]

$$\frac{d[m\dot{x}(t)]}{dt}=[-\nabla V(x,t)-\nabla Q(x,t)]|_{x(t)}.\qquad (4)$$

Equation (4) shows that, at each Bohmian position $x(t)$, in addition to the usual classical force $-\nabla V(x,t)$, the particle also experiences what Bohm called a quantum force $-\nabla Q(x,t)$ where the quantum potential [1,2]

$$Q(x,t)=-\frac{\hbar^2}{2m}\frac{\nabla^2 R(x,t)}{R(x,t)}\qquad (5)$$

is determined by the amplitude $R(x,t)$ of the quantum wave function in Eq. (2).

Equations (1) and (4) are two equivalent [1] versions of Bohm's equation of motion provided that Eq. (4) is subject to the constraint $p(t=0)=\nabla S(x,t=0)|_{x_0}$ for the initial momentum. However, it easier to solve Eq. (1) to obtain the position and momentum of the particle in practice. Largely ignored since its inception, Bohm's interpretation, which reproduces [1] precisely all the predictions of the standard Copenhagen interpretation, has recently [3–6] gained a more widespread interest and acceptance.

Some features of the quantum potential have been discussed by Bohm [1] and also by Bohm and Hiley [2]. In this paper, we focus on the temporal behavior of Bohm's quantum force experienced by the particle at the Bohmian position:

$$F_Q(t)\equiv-\nabla Q(x,t)|_{x(t)}.\qquad (6)$$

In general, $F_Q(t)$ depends on the system parameters, the initial wave function, and initial Bohmian position. The explicit dependence of $F_Q(t)$ on time is known, so far, only in a few cases where analytical expressions can be obtained for the amplitude [this determines the quantum potential $Q(x,t)$, Eq. (5)] and phase [this determines the Bohmian position $x(t)$, Eq. (1)] of the time-dependent wave function. One such case is a system with a time-independent potential $V(x)$ that supports a set of real, bound-state energy eigenfunctions $\phi_n(x)$ with corresponding energies E_n. If the initial wave function is any one of these eigenfunctions, then

$$\psi(x,t)=\varphi_n(x)\exp(-iE_nt/\hbar).\qquad (7)$$

For this stationary state [1], the Bohmian position at time t is equal to its initial position

$$x(t)=x_0,\qquad (8)$$

and, the quantum force is time independent, equal in magnitude but opposite in direction to the time-independent classical force. Thus Eq. (6) gives

$$F_Q(t)=\nabla V(x)|_{x(t)=x_0}=\text{const.}\qquad (9)$$

 ©2001 The American Physical Society

Another case is the free particle: if the initial wave function is an energy eigenfunction (or momentum eigenfunction) $\phi_k(x)=Ae^{ikx}$ with energy $E_k=\hbar^2k^2/2m$, then

$$\psi(x,t)=A\,\exp[i(kx-E_kt/\hbar)]. \tag{10}$$

Since the amplitude of this stationary state is independent of x, the quantum potential vanishes for all times [7], and thus

$$F_Q(t)=0. \tag{11}$$

For the harmonic oscillator [8] and free particle [9,10], the explicit dependence of $F_Q(t)$ on time is also known for wave packets. For the harmonic oscillator [8], if the initial wave function is a minimum-uncertainty Gaussian wave packet with position standard deviation $\sqrt{\hbar/2m\omega}$, then the wave packet remains Gaussian without spreading in position and momentum:

$$\psi(x,t)=\left(\frac{m\omega}{\pi\hbar}\right)^{1/4}\exp\left[-\frac{m\omega}{2\hbar}(x-a\cos\omega t)^2\right]\times\exp\left\{-\frac{i}{2}\left[\omega t+\frac{m\omega}{\hbar}\left(2ax\sin\omega t-\frac{1}{2}a^2\sin 2\omega t\right)\right]\right\}. \tag{12}$$

For this Gaussian wave packet, initially centered at a in position and 0 in momentum, the Bohmian position is given by [8]

$$x(t)=x_0+a\cos\omega t-a, \tag{13}$$

and the quantum force is given by [8]

$$-\nabla Q=m\omega^2(x-a\cos\omega t), \tag{14}$$

and therefore Eq. (6) gives

$$F_Q(t)=m\omega^2(x_0-a)=\text{const.} \tag{15}$$

From Eq. (15), we see that if $x_0=a$, then $F_Q(t)=0$.

For the free particle [9], if the initial wave function is a minimum-uncertainty Gaussian wave packet, then the wave packet remains Gaussian that spreads in position but not in momentum:

$$\psi(x,t)=\left(\frac{1}{2\pi\sigma_t^2}\right)^{1/4}\exp\left[\frac{-(x-ut)^2}{4\sigma_t^2}\right]\times\exp\left\{i\left[\frac{f(t)(x-ut)^2}{4\sigma_t^2}+k\left(x-\frac{ut}{2}\right)-\frac{1}{2}\tan^{-1}[f(t)]\right]\right\}, \tag{16}$$

where $u=\hbar k/m$, $f(t)=\hbar t/2m\sigma_0^2$, and $\sigma_t^2=\sigma_0^2[1+f^2(t)]$ is the position variance at time t. For this Gaussian wave packet, initially centered at 0 in position and $\hbar k$ in momentum, the Bohmian position is given by [9]

$$x(t)=ut+x_0[1+f^2(t)]^{1/2}, \tag{17}$$

and the quantum force is given by [9]

$$-\nabla Q=\frac{\hbar^2}{4m\sigma_t^4}(x-ut), \tag{18}$$

and therefore Eq. (6) gives

$$F_Q(t)=\frac{\hbar^2x_0}{4m\sigma_0^4\left(1+\dfrac{\hbar^2t^2}{4m^2\sigma_0^4}\right)^{3/2}}. \tag{19}$$

From Eq. (19) we see that if $x_0=0$, then $F_Q(t)=0$; if $x_0>0$ ($x_0<0$), then $F_Q(t)$ decreases (increases) monotonically with time and approaches zero as t approaches infinity. For the free particle [10], if the initial wave function is

$$\psi(x,0)=\text{Ai}(Bx/\hbar^{2/3}), \tag{20}$$

where B is a constant and Ai is the Airy function, then

$$\psi(x,t)=\text{Ai}[(B/\hbar^{2/3})(x-B^3t^2/4m^2)]\times\exp[(iB^3t/2m\hbar)(x-B^3t^2/6m^2)]. \tag{21}$$

For this wave packet that propagates without spreading in position [10]

$$F_Q(t)=\frac{B^3}{2m}\bigg|_{x(t)}=\frac{B^3}{2m}=\text{const.} \tag{22}$$

In the few cases above where the explicit dependence of $F_Q(t)$ on time is known, $F_Q(t)$ is either independent of time or monotonically decreasing or increasing with time. In this paper, we show that a very different and interesting behavior of $F_Q(t)$ occurs in the periodically delta-kicked plane pendulum system with Hamiltonian [11]

$$H(\theta,t)=\frac{P^2}{2mL^2}-mL^2\omega_0^2\cos\theta\sum_{j=-\infty}^{\infty}\delta\left(j-\frac{t}{T}\right), \tag{23}$$

where T is the kicking period, $\omega_0=\sqrt{g/L}$ is the small amplitude frequency of the unperturbed pendulum, g is the acceleration due to gravity, L and m are, respectively, the length and mass of the pendulum. For this well-known prototypical Hamiltonian dynamical system that exhibits classical chaos, both the time-dependent Schrödinger equation and Bohm's equation of motion have to be integrated numerically in general to yield the wave function and Bohmian angle, respectively. Details of the numerical integrations are given in Sec. II. Just before each instantaneous gravitational kick $n=1,2\ldots$, the quantum force is determined from the wave function and evaluated at the Bohmian angle to yield a quantum force time-series $F_Q(n-1)$ with uniform time intervals. The results of our analysis of these quantum-force time series are presented and discussed in Sec. III. In Sec. IV, we conclude from our findings, offer a conjecture on which other systems would exhibit similar quantum-force time-series properties as the kicked pendulum, and finally describe a new alternative method of calculating the quantum probability density of a particle's position implied by those quantum-force properties.

II. TIME-DEPENDENT SCHRÖDINGER EQUATION AND BOHM'S EQUATION OF MOTION

For the kicked pendulum, the time-dependent Schrödinger equation can be integrated analytically exactly to yield a mapping [12] of the wave function, from just before the nth kick to just before the $(n+1)$th kick, with two dimensionless parameters $\kappa = a/\hbar$ and $\tau = b\hbar$, where $a = mLgT$ and $b = T/mL^2$. Substituting the wave function expansion in free-rotor energy eigenstates

$$\psi(\theta,t) = \frac{1}{\sqrt{2\pi}} \sum_{k=-\infty}^{\infty} A_k(t) e^{ik\theta} \tag{24}$$

into the wave function mapping yields a mapping [12] of the wave function expansion coefficients from just before the nth kick to just before the $(n+1)$th kick, $n = 1,2,\ldots$:

$$A_k(n) = \exp\left[-i\frac{k^2\tau}{2}\right] \sum_{j=-\infty}^{\infty} A_j(n-1) i^{k-j} J_{k-j}(\kappa), \tag{25}$$

where J is a Bessel function of the first kind of integer order.

Bohm's equation of motion

$$\frac{d\theta}{dt} \equiv \frac{1}{mL^2}\frac{\partial S(\theta,t)}{\partial\theta} = \frac{\hbar}{mL^2}\mathrm{Im}\left[\frac{1}{\psi(\theta,t)}\frac{\partial\psi(\theta,t)}{\partial\theta}\right]$$
$$= \frac{b\hbar}{T}\mathrm{Im}\left[\frac{1}{\psi(\theta,t)}\frac{\partial\psi(\theta,t)}{\partial\theta}\right] \tag{26}$$

is integrated numerically to obtain the Bohmian angle just before the $(n+1)$th kick given the initial angle just before the nth kick. Numerical integration of the first-order differential equation (26) is done using the adaptive-step-size, fourth-fifth-order, Runge-Kutta-Fehlberg method, where the wavefunction is calculated with Eq. (24) using the expansion coefficients from the mapping Eq. (25).

All numerical calculations were performed in double precision. To ensure that a sufficient number of wave-function expansion coefficients were time evolved using the mapping Eq. (25), the normalization of the wave function, i.e., $\Sigma|A_k|^2 = 1$, was monitored. For the results presented in the next section, the normalization is satisfied to at least 13 decimal places. In the numerical integration of Bohm's equation of motion Eq. (26), convergence was checked by changing the relative and absolute error tolerances.

III. RESULTS AND DISCUSSION

Just before each instantaneous gravitational kick $n = 1,2,\ldots$, the quantum force is determined from the wave function and evaluated at the Bohmian angle to yield a quantum-force time series

$$F_Q(n-1) = -\nabla Q(\theta, n-1)|_{\theta(n-1)} \tag{27}$$

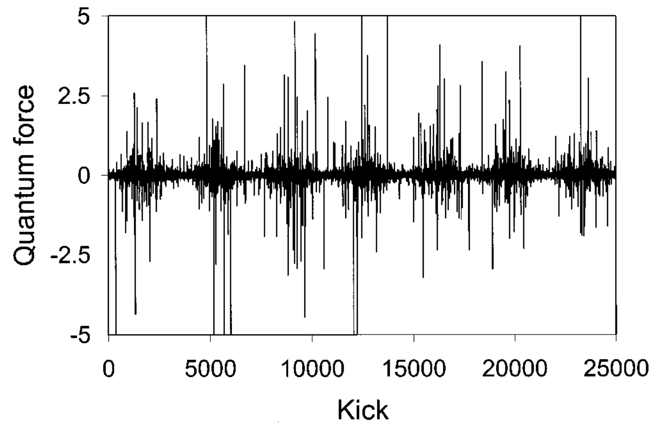

FIG. 1. A quantum-force time series: the quantum force (in arbitrary unit) just before each kick is plotted against the kick number.

where the time interval between successive values is the kicking period T.

A quantum-force time-series $F_Q(n-1)$ is shown in Fig. 1. In this case, the system parameters are $a = mLgT = 0.005$ and $b = T/mL^2 = 50$ where the kicking period $T = 1$. We chose $\hbar = 0.0001$ to keep the number of expansion coefficients required for accurate wave-function representation computationally manageable. The initial wave-function expansion coefficients is Gaussian centered at k_0:

$$A_k(0) = \left(\frac{2\sigma_0^2}{\pi}\right)^{1/4} \exp[-\sigma_0^2(k-k_0)^2]\exp(-ik\theta_0). \tag{28}$$

For $\sigma_0 \ll 1$, these expansion coefficients yield an initial wave function that is [12], to a very good approximation, a very well localized, minimum-uncertainty Gaussian wave packet in the angle interval $[0,2\pi]$ with mean values

$$\langle\theta(0)\rangle \approx \theta_0, \quad \langle P(0)\rangle \approx \hbar k_0 \tag{29}$$

and variances

$$\sigma_\theta^2(0) \approx \sigma_0^2, \quad \sigma_P^2(0) \approx \frac{\hbar^2}{4\sigma_0^2} \tag{30}$$

for the angle and angular momentum respectively. For the time series in Fig. 1, the initial wave-function parameters in Eq. (28) are $\sigma_0 = 0.01$, $\theta_0 = \pi$, and $k_0 = 3142$. The initial Bohmian angle is set to θ_0. All quantities with dimensions are in arbitrary units.

The quantum-force time series in Fig. 1 exhibit several striking qualitative features: (i) the quantum force exhibits cyclic but *non*-periodic behavior; (ii) large positive and negative values of the quantum force occur repeatedly, and (iii) these large values of the quantum force cluster together in distinct bunches. These qualitative features of the quantum-force time series have been observed in financial time series of stock-price changes [13,14] and currency-exchange rate changes [14].

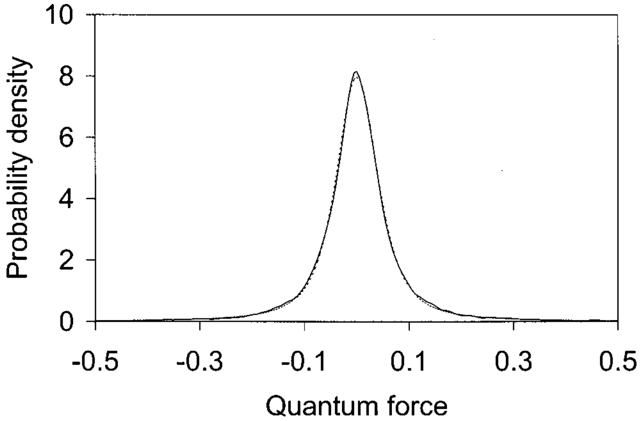

FIG. 2. Probability density function of the quantum-force data set in Fig. 1: smoothed data density (solid line) and fitted stable density (dotted line). The fitted stable density is essentially symmetric ($\beta = 0.0099$) with a non-Gaussian characteristic exponent $\alpha = 1.28$.

Stock-price changes and currency-exchange rate changes [15,16], and other empirical time series such as changes in the time interval between sequential human heart beats [17] and changes in the time interval between sequential water drops in a leaky faucet [18], were found to be stable, but non-Gaussian, distributed. The class of stable distributions [16,19] is characterized by four parameters: characteristic exponent $\alpha \in (0,2]$, skewness $\beta \in [-1,1]$ (symmetric if $\beta = 0$), scale $\sigma \in (0,\infty)$, and location $\mu \in (-\infty,\infty)$. The Gaussian ($\alpha = 2$) is the only member of this class of distributions with a finite variance; all other members have infinite variance and heavier density tails than the Gaussian.

Motivated by the qualitative similarity between the quantum-force time series in Fig. 1 and the time series of stock-price changes and currency-exchange rate changes, we fitted the large quantum-force data set (25001 values) in Fig. 1 with a stable distribution using Nolan's STABLE program [20]. The fit, which employs the maximum likelihood method [21] based on reliable computations [22] of stable densities, produced the following stable parameters in the S^0 parametrization [23]: $\alpha = 1.28$, $\beta = 0.0099$, $\sigma = 0.037$, and $\mu = 0.000\,28$. A visual comparison of the smoothed data density with the fitted stable density in Fig. 2 shows that, qualitatively, the symmetric, non-Gaussian stable fit is good. In addition, a quantitative goodness-of-fit test is provided by the modified PP (percent-percent) plot [24] in Fig. 3. The acceptance region, based on a goodness-of-fit statistic that is analogous to the Kolmogorov-Smirnov statistic, can be added to the PP plot by drawing two straight lines spaced a uniform distance above and below the diagonal [24]. However, this is not necessary since the PP plot in Fig. 3 is essentially on the diagonal, and thus, to a high level of significance, the quantum-force data set in Fig. 1 is non-Gaussian stable distributed. Furthermore, we found that different subsets of the full data set are identically distributed as the full set.

In addition, we have calculated the power spectrum of the quantum-force time series in Fig. 1 using the maximum entropy (all poles) method [25]. The power spectrum, shown in

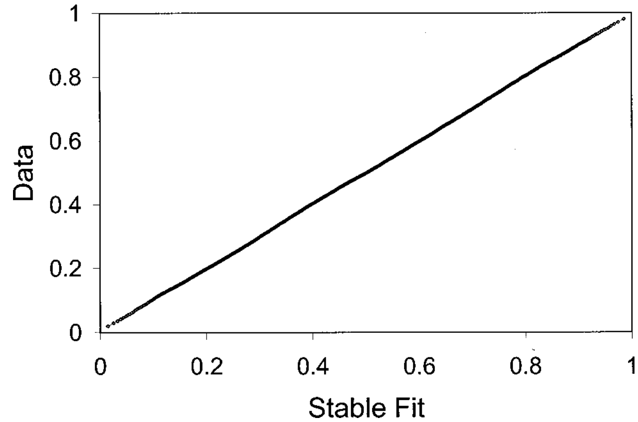

FIG. 3. Modified PP (percent-percent) plot for the quantum-force data set in Fig. 1.

Fig. 4, is flat. Furthermore, the spectrum for different subsets of the data in Fig. 1 does not differ significantly from the one in Fig. 4.

We have also, for the kicked pendulum, studied the quantum-force time series $F_Q(n-1)$ for an extensive *variety* of system parameters, initial wave functions, and initial Bohmian angles. For the system parameters, we have used values of $a = mLgT$ and $b = T/mL^2$, where the dimensionless product *ab*, which determines the degree of chaos in *classical* phase space [11], ranges from 10^{-4} to 1 (the transition from local or weak chaos to global or strong chaos occurs at $ab \approx 0.9716$ [11]). For the initial wave function, we have (i) varied the parameters σ_0, θ_0, and k_0 of the expansion coefficients in Eq. (28), (ii) used a set of N expansion coefficients of equal amplitude $1/\sqrt{N}$, and (iii) used different mth free-rotor eigenstate as the initial wave function, i.e., $A_k(0) = \delta_{\mathrm{km}}$. In *all* these diverse cases (different system parameters, initial wave functions, initial Bohmian angles) involving nonstationary states, we find that the quantum-force time series has the same qualitative features as the time series in Fig. 1. And in each case, using the density plot and modified PP plot diagnostics, we find that the quantum-force time series is also non-Gaussian stable distributed (for both

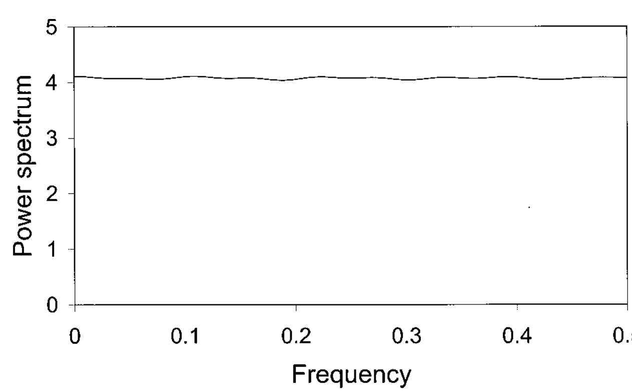

FIG. 4. Power spectrum, calculated using 20 poles, of the quantum-force time series in Fig. 1 versus frequency (in arbitrary units) up to the Nyquist frequency [defined as $1/(2\Delta)$, where Δ is the sampling interval [25]] of 0.5.

first-order and second-order densities) but with, generally, different parameters. We find that, however, for fixed system parameters and fixed initial wave function, the stable parameters remain the same for different initial Bohmian angles. And finally, in each case, we find that the power spectrum of the quantum-force time series is flat whose value is, for fixed system parameters and fixed initial wave function, independent of the initial Bohmian angle.

There is one exception, we know of, to our findings above. For $\tau = b\hbar = 4\pi$, it can be shown, using the wave-function expansion, Eq. (24), and expansion-coefficient mapping, Eq. (25), that the wave function just before kick $n = 1,2\ldots$ is given by [26]

$$\psi(\theta, n-1) = \exp[i\kappa(\cos\theta)(n-1)]\psi(\theta,0). \tag{31}$$

If the initial wave function is an mth free-rotor eigenstate, then

$$\psi(\theta, n-1) = \frac{1}{\sqrt{2\pi}}\exp[i\kappa(\cos\theta)(n-1)]\exp[im\theta]. \tag{32}$$

Since the amplitude of this wave function is independent of θ, the quantum potential $Q(\theta, n-1) = 0$ and thus $F_Q(n-1) = 0$ for $n = 1,2\ldots.$

IV. CONCLUSION, CONJECTURE, AND IMPLICATION

Based on our numerical study, we conclude that, for the kicked pendulum, Bohm's quantum-force time series for nonstationary states is *typically* or *generically* (i.e., exceptions are very rare) non-Gaussian stable distributed with a flat power spectrum. For fixed system parameters and initial wave function, the stable parameters and the constant value of the power spectrum are independent of the initial Bohmian angular position.

We conjecture (hypothesize) that the above properties of the quantum-force time series are also typical or generic for other classically chaotic Hamiltonian dynamical systems since the kicked pendulum is a prototypical [11] member of this class of systems. We do not expect the same to be true for classically nonchaotic Hamiltonian dynamical systems since in two such systems: free particle and harmonic oscillator, the quantum-force time series for nonstationary states is neither non-Gaussian stable distributed nor does it have a flat power spectrum (see Introduction).

In general, the quantum probability density of the particle's position can be calculated from the quantum time-dependent wave function, i.e., $|\psi(x,t)|^2$ (Method 1), or [1] as the position probability density of an ensemble of Bohmian trajectories, where each member of the ensemble is time evolved using Eqs. (1) or (4) (Method 2). These two methods give the same results for all times if the position probability density of the ensemble equals $|\psi(x,0)|^2$ initially [1]. In Method 2, in order to time evolve each member of the ensemble using Eqs. (1) or (4), the time-dependent Schrödinger's equation also has to be solved to obtain the phase or amplitude of the wave function.

In the case where the quantum wave function is a nonstationary state and the time series of $F_Q(t) \equiv -\nabla Q(x,t)|_{x(t)}$ in Eq. (4) is, for each member of the ensemble, identically non-Gaussian stable distributed with a flat power spectrum, if each member of the ensemble is instead time evolved using a *stochastic* differential equation

$$\frac{d[m\dot{x}(t)]}{dt} = -\boldsymbol{\nabla} V(x,t)|_{x(t)} + \tilde{F}_Q(t) \tag{33}$$

obtained from Eq. (4), where $F_Q(t)$ is replaced by the appropriate stationary non-Gaussian stable white (flat power spectrum) *random* force $\tilde{F}_Q(t)$, then the position probability density of the ensemble is equal to the density obtained in Method 2 for all times, if they are equal initially. This equivalence holds because in Method 2, $F_Q(t)$ in Eq. (4) for each member of the ensemble is a particular realization of the stationary non-Gaussian stable white random force $\tilde{F}_Q(t)$. As a consequence of this equivalence and the equivalence between Methods 1 and 2 above, the position probability density of an ensemble, where each member time evolves according to Eq. (33), is equal to $|\psi(x,t)|^2$ for all times if the density is equal to $|\psi(x,0)|^2$ initially. Note that, in this third method of calculating the quantum probability density of a particle's position, only one equation needs to be solved as in Method 1, but it is a stochastic differential equation (33) instead of Schrödinger's partial differential equation. In contrast, two equations, Schrödinger's equation and an ordinary differential equation, Eqs. (1) or (4), have to be solved in Method 2.

A direct proof, instead of the indirect proof in the previous paragraph, of the equivalence between the stochastic differential equation (33) and the time-dependent Schrödinger's equation, is planned for a future publication, together with numerical examples for the kicked pendulum.

[1] D. Bohm, Phys. Rev. **85**, 166 (1952); **85**, 180 (1952).

[2] D. Bohm and B. J. Hiley, *The Undivided Universe* (Routledge, London, 1993), Chap. 3.

[3] P. R. Holland, *The Quantum Theory of Motion* (Cambridge University, Cambridge, 1993).

[4] J. T. Cushing, *Quantum Mechanics: Historical Contingency and the Copenhagen Hegemony* (University of Chicago, Chicago, 1994).

[5] D. Z. Albert, Sci. Am. **274** (5), 32 (1994).

[6] S. Goldstein, Phys. Today **51** (4), 38 (1998). See also letters in response to this article in Phys. Today **52** (2), 15 (1999) by J. L. Anderson (p. 89), W. G. Hoover (p. 90), and H. M. Bradford (p. 92).

[7] Reference [3], Sec. 4.2.

[8] Reference [3], Sec. 4.9 and Sec. 6.6.1.

[9] Reference [3], Sec. 4.7.

[10] Reference [3], Sec. 4.10.

[11] B. V. Chirikov, Phys. Rep. **52**, 263 (1979).

[12] R. F. Fox and B. L. Lan, Phys. Rev. A **41**, 2952 (1990).

[13] B. B. Mandelbrot, *Fractals and Scaling in Finance: Discontinuity, Concentration, Risk* (Springer-Verlag, New York, 1997), pp. 18, 26, 27.

[14] B. B. Mandelbrot, Sci. Am. **279** (2), 50 (1999).

[15] Reference [13], part IV.

[16] J. H. McCulloch, in *Statistical Methods in Finance, Handbook of Statistics*, edited by G. S. Maddala and C. R. Rao (North-Holland, New York, 1996), Vol. 14.

[17] C.-K. Peng, J. Mietus, J. M. Hausdorff, S. Havlin, H. E. Stanley, and A. L. Goldberger, Phys. Rev. Lett. **70**, 1343 (1993).

[18] T. J. P. Penna, P. M. C. de Oliveira, J. C. Sartorelli, W. M. Gonçalves, and R. D. Pinto, Phys. Rev. E **52**, R2168 (1995).

[19] Information on the stable distributions is scattered in Ref. [13] and is also in some recent books: G. Samorodnitsky and M. S. Taqqu, *Stable Non-Gaussian Random Processes* (Chapman and Hall, New York, 1994); A. Janicki and A. Weron, *Simulation and Chaotic Behavior of α-Stable Stochastic Processes* (Marcel-Dekker, New York, 1994).

[20] J. P. Nolan, in *A Practical Guide to Heavy Tails: Statistical Techniques and Applications*, edited by R. J. Adler, R. E. Feldman, and M. S. Taqqu (Birkhäuser, Boston, 1998). The STABLE program can be downloaded from www.cas.american.edu/~jpnolan

[21] J. P. Nolan, *Maximum Likelihood Estimation and Diagnostics for Stable Distributions* (American University, Washington, DC, 1998), available at www.cas.american.edu/~jpnolan

[22] J. P. Nolan, Comm. Stat.-Stoch. Models **13**, 759 (1997).

[23] J. P. Nolan, Stat. Prob. Lett. **38**, 187 (1998).

[24] J. R. Michael, Biometrika **70**, 11 (1983). See also Ref. [21].

[25] W. H. Press, B. P. Flannery, S. A. Teukolsky, and W. T. Vetterling, *Numerical Recipes in C: The Art of Scientific Computing* (Cambridge University, Cambridge, 1988), Chap. 12.8.

[26] F. M. Izrailev and D. L. Shepelyansky, Theor. Math. Phys. **43**, 553 (1980).